

# Influence of the Dispersants in Gelcasting of Nanosized TiN

Rolf Wäsche & Gabriele Steinborn

Federal Institute for Materials Research and Testing (BAM), D-12200 Berlin, Germany

(Received 15 September 1995; accepted 23 July 1996)

## Abstract

*The gelcasting process for shaping of plasma synthesized nanosized TiN with regard to the dispersion behaviour and the resultant microstructures has been investigated. The dispersion behaviour of the powder and rheology of the slurries under the influence of three different dispersants have been studied as a function of pH. Solid content of the slurries was up to 22 vol%. The isoelectric points as measured by the streaming potential method were found to be at a pH of 3.7 and lower. Sintering of the dried and debindered green bodies was carried out in a N<sub>2</sub> atmosphere with the application of 50 bar gas pressure in the final sintering stage leading to densities of 95.5%. Resulting microstructures are strongly dependent on the dispersant used. © 1996 Elsevier Science Limited.*

*Der Polymerschlickergießprozeß ist für die Formgebung von nanokristallinem TiN, das durch einen plasmainduzierten Gasphasenreaktionsprozeß hergestellt wurde, untersucht worden. Dabei standen das Dispersionsverhalten und die entstehenden Mikrogefüge im Vordergrund. Unter Verwendung von drei unterschiedlichen Dispergatoren sind das Dispersionsverhalten des Pulvers und die rheologischen Eigenschaften der Schlicker in Abhängigkeit vom pH-Wert untersucht worden. Der Feststoffgehalt der Schlicker betrug bis zu 22 vol%. Die isoelektrischen Punkte, bestimmt mit der Methode der Strömungspotentialmessung, lagen bei pH-Werten von 3.7 und niedriger. Die Sinterung der getrockneten und entbinderten Grünkörper wurde unter einer N<sub>2</sub>-Atmosphäre in einer Gasdrucksinteranlage durchgeführt, wobei in der letzten Sinterphase der N<sub>2</sub>-Druck auf 50 bar erhöht wurde. Die erreichten Sinterdichten betragen bis zu 95.5%, wobei die Homogenität der Gefüge stark vom verwendeten Dispergator abhängig war.*

## 1 Introduction

Gelcasting is a new forming method for the shaping of ceramic green bodies. As shown in several publications this process is applicable to shaping of both monolithic ceramics and composite materials.<sup>1–5</sup> In this process the ceramic powder is dispersed in a liquid medium in order to obtain a high solids loaded slurry which is then cast into a mold of the desired shape. In aqueous gelcasting the interaction between the particle surface and water as the dispersing medium is of crucial importance. In most cases a surface modifying agent must be added in order to reduce the interparticle attractive forces and to obtain colloidally stable, homogeneous slurries characterised by a viscosity low enough for casting and for proper de-airing prior to casting. Since the rheological behaviour of slurries with high solids loading tends to be non-Newtonian<sup>6</sup> the rheology of the slurry is important to investigate. The characterisation of the electrokinetic behaviour and the corresponding isoelectric points (IEP) is important for working at pH values where the colloidal stability of the slurries is high enough. In the present work the main objective was the screening of the influence of commercially available dispersants for dispersing nanocrystalline titanium nitride in water and the investigation of the gelcasting process for this material.

## 2 Experimental Procedures

The gelcasting process flow chart is shown in Fig. 1. The slurries were prepared by suspending the powder in distilled water with different dispersants. The dispersants used were PC 33, a polycarbonate; CE 64, a citric acid derivative and KV

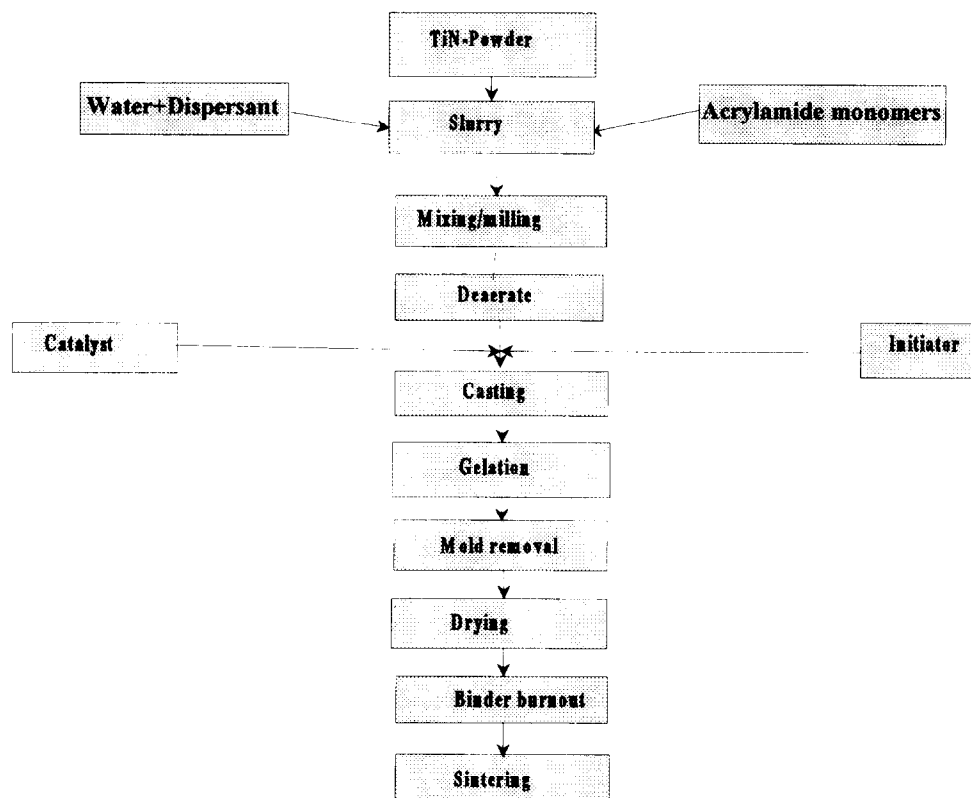


Fig. 1. Gelcasting process flowchart.

5088, an aminoalcohol (Zschimmer and Schwartz, Lahnstein, Germany). Prior to measurement and casting the slurries were mechanically stirred, ultrasonicated and degassed under vacuum. The electrokinetic characterisation and the measurement of the IEP were carried out with the particle charge detector PCD 02 (Malvern, Munich, Germany) according to the streaming potential method.<sup>9</sup> The adjustment of the pH was done using hydrochloric acid. For these measurements a slurry with 10 wt% TiN was prepared. Dispersants have been added at a concentration of 0.6 % relative to the powder content. The viscosity measurements were carried out by means of a rotary viscosimeter (Haake Rotovisko RV 3) with a conical cylinder and cup geometry (measuring head DMK 50/500, measuring system MV-DIN), according to the DIN Norm 53019-TO1-80, in the shear rate range from 1 to 1000 s<sup>-1</sup>. All measurements were carried out at a temperature of 25°C in a thermostated measuring device.

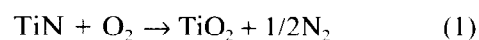
Sintering has been carried out in nitrogen with a heating rate of 10 K/min to the sintering temperature of 1550°C<sup>8,14</sup> and with the application of 50 bar gas pressure in the final sintering stage. The consolidation of the samples during sintering was observed and controlled by means of an integrated high temperature dilatometer, placed inside the sintering chamber of the gas pressure sintering device. Temperature, gas pressure, shrinkage and shrinkage velocity were recorded for the analysis

of the sintering process. Binder burnout took place prior to sintering in a special debinding furnace at temperatures of 700°C under a nitrogen atmosphere. The corresponding green densities of the cast dried bodies were measured to be about 26% of the theoretical density. Green bodies made by die-pressing under a pressure of 100 MPa had a green density of 34%.

### 3 Results and Discussion

#### 3.1 Powder characterisation

Table 1 gives an overview of the main powder data. The powder, which was prepared via a gas phase reaction process from gaseous precursors,<sup>7,13</sup> contains spherical particles the primary diameter of which is in the range of about 15–30 nm. These primary particles cluster together to form irregularly shaped powder agglomerates. The diameter of these agglomerates may reach several hundreds of nanometers as may be seen from Fig. 2. The specific surface as measured by the BET method was found to be about 36 m<sup>2</sup>/g. The chlorine content, which is a remainder of the manufacturing process, was found to be 0.5 wt%. The oxygen content was found to be 7.1 wt% and is due to the thermodynamic instability of TiN towards oxygen. TiO<sub>2</sub> is formed by the oxidation of TiN through the following reaction:<sup>10,11</sup>



The powders in use were already contaminated by air prior to shipping, so that a spontaneous oxidation reaction and a burning of the powders during handling was not observed. The investigation of the oxidation behaviour showed that complete oxidation of the powder starts at temperatures of about 250°C and is completed at 400°C leading to

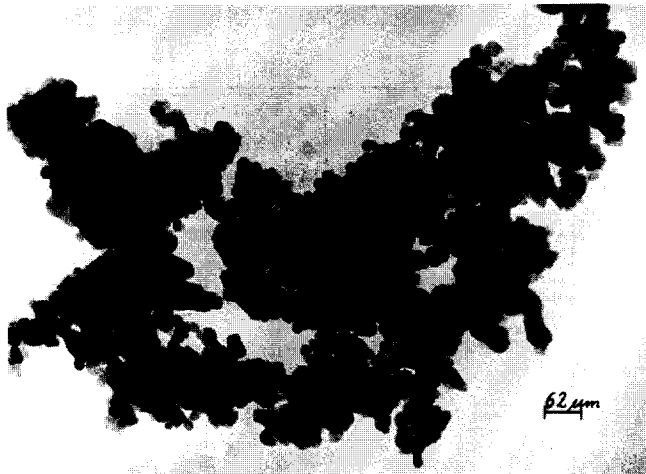


Fig. 2. Transmission electron micrograph (TEM) of TiN powder.

the rutile phase which is in good agreement with the results of Gogotsy and Yoshimura.<sup>11</sup> XPS measurements have also shown, that the powder particle surface is covered by an oxide layer which protects the particles at room temperature from further oxidation. Further oxidation of the powders during handling in air or during aqueous processing during long time periods was not observed. These oxide phases are at least partly crystalline as indicated by the X-ray diagram of the powder shown in Fig. 3. Beside the peaks for the anatase (101) and (200) reflections there is another reflection at an angle of  $2\theta = 34.4^\circ$ , which is assumed to be caused by the presence of a substoichiometric  $\text{TiO}_2$  phase.<sup>9</sup> This phase disappears during the sintering step whereafter with X-ray diffraction only anatase could be identified as a second phase in the microstructure.

### 3.2 Electrokinetic characterisation and rheology of the slurries

Figure 4 shows the measurement of the PCD streaming potential as a function of the pH for pure titanium nitride and for TiN with different

Table 1. Characterisation of the TiN-powder

Manufacturer	Tioxide Ltd, Billingham, UK
Phase content	Titanium nitride (Osbornite), traces of $\text{TiO}_2$
Spec. surface ( $\text{m}^2/\text{g}$ )	36
Mean grain size (nm)	15–30
Oxygen content (wt%)	7.1
Chlorine content (wt%)	0.5

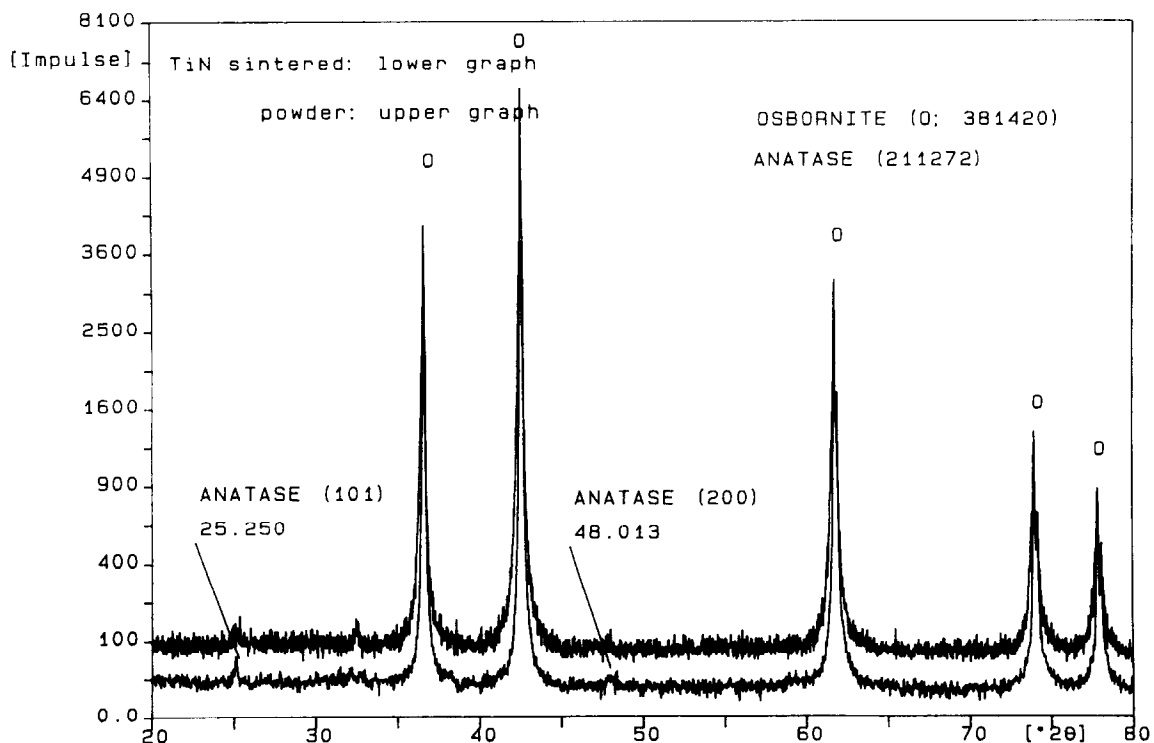
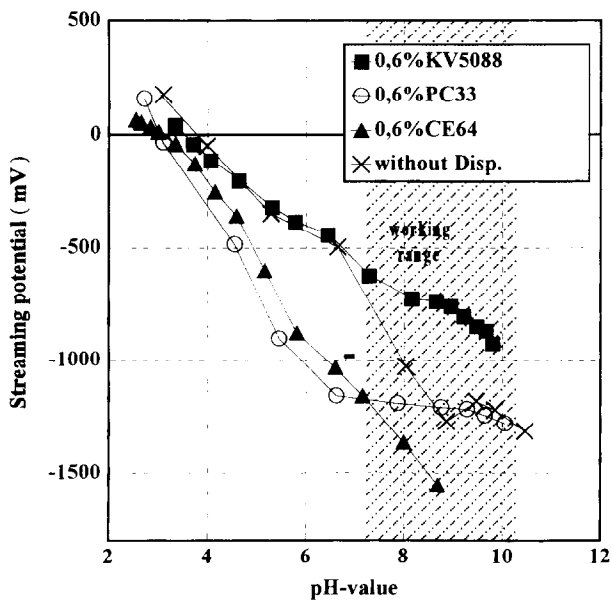
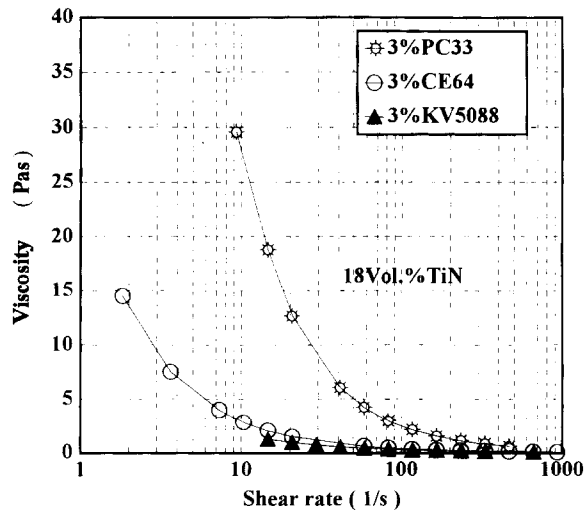


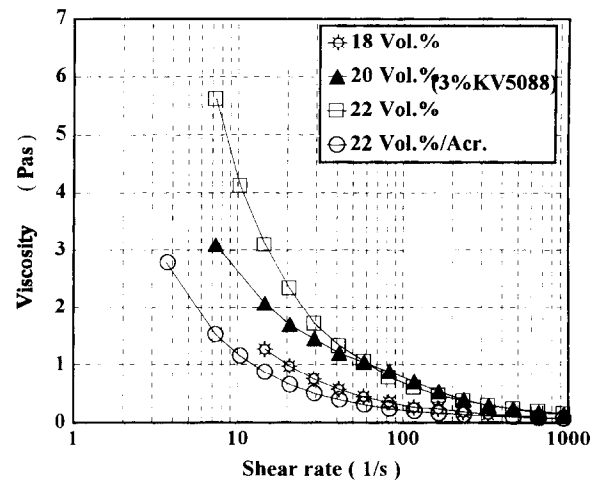
Fig. 3. X-ray diffraction diagram of TiN powder.

**Table 2.** Influence of dispersant on the limit of solids loading and the sintered density

Dispersant Chemical classification	PC 33 Polycarbonate	CE 64 Citric acid derivative	KV 5088 Aminoalcohol
Maximum of solids loading (vol %)	19	20	22
Sintered density (%)	70	88	95.5

**Fig. 4.** Streaming potential and isoelectric points (IEP) as a function of pH for TiN slurries with different dispersants (solid loading 10 wt%)**Fig. 5.** Viscosity as a function of shear rate for TiN slurries with different dispersants.

dispersants as shown in Table 2. The corresponding IEPs have been found in all cases to be below pH 3.7 with a tendency to shift the IEP to lower pH values when a dispersant was added. Accordingly the working range for the slurries was in the basic side of the pH scale at values between pH 8 and 10. Since the particle charge was highest in

**Fig. 6.** Viscosity as a function of shear rate for TiN slurries with KV 5088 as dispersant and with different solids loading.

this range, the corresponding slurries were also most stable with low viscosity values.

Although the electrokinetic behaviour of the three dispersants used in this investigation is very similar, the dispersing abilities and results are quite different. The best dispersing behaviour was found with the aminoalcohol KV 5088. This dispersant allowed the highest solids loading and as later described in greater detail also the most homogeneous microstructure and the highest sintering density.

Figure 5 shows the viscosity as a function of the shear rate for TiN slurries with 18 vol% and different dispersants. With solids loading in this range slurries without any dispersant could not be prepared. As observed in all slurries used in this investigation the viscosity is strongly decreasing with increasing shear rate and shows the shear-thinning effect. Best results were shown by the slurry with KV 5088 as dispersant.

Figure 6 characterises the effect of increasing solids loading on the viscosity, but all with dispersant KV 5088. As found also in the viscous behaviour of alumina powders,<sup>1,5</sup> at a given shear rate the viscosity increases exponentially with increasing solid content of the slurry. However, in the system investigated here, the presence of the acrylamide monomers had a beneficial effect with regard to lowering the viscosity by about a factor of three but without changing the flow behaviour.

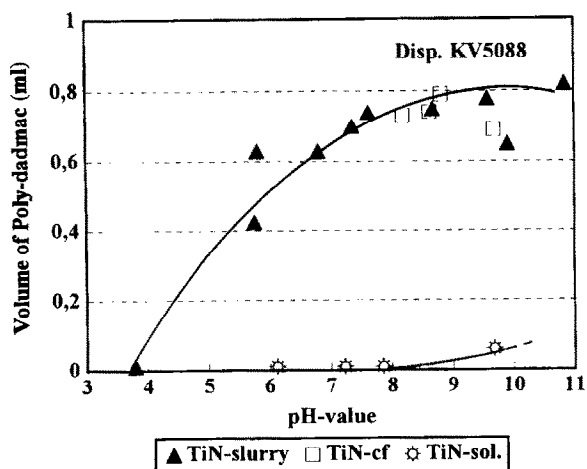
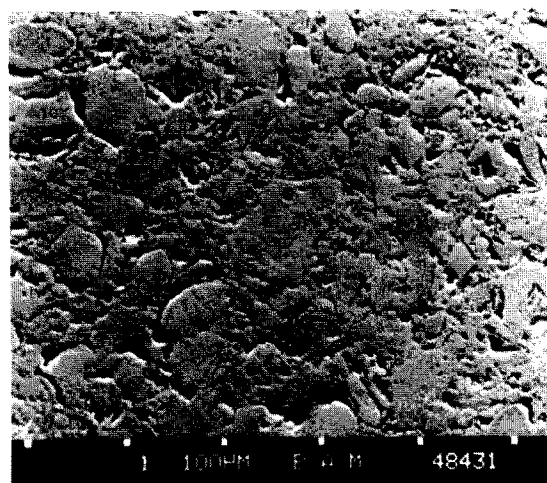


Fig. 7. Titration volume of Polydadmac as a function of pH for the TiN slurry, centrifuged and redispersed powder (TiN-cf) and the centrifuged solvent (TiN-sol.)

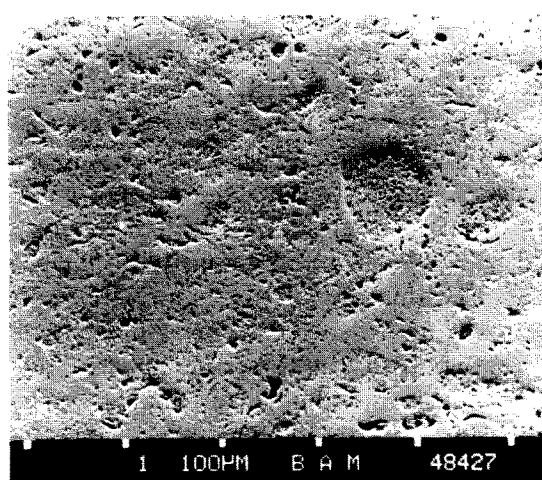
Ball milling of the slurry improved the rheology also, but to a minor extent. In some cases ultrasonic treatment of the slurries turned out to be problematic because of the start of polymerisation before casting. This phenomenon is already known for highly activated fine particle surfaces as described during the gelcasting process of silicon.<sup>12</sup>

### 3.3 Adsorption behaviour

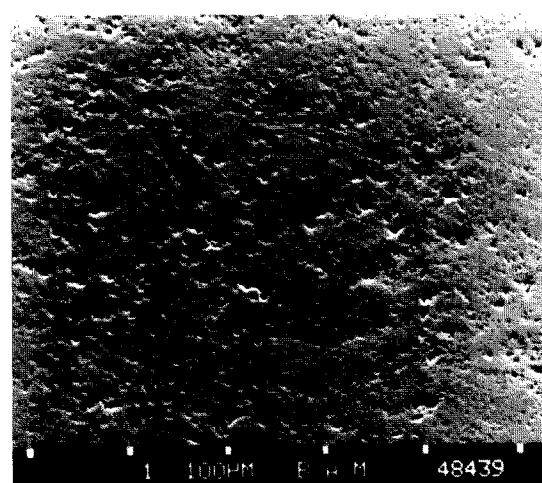
In order to investigate the adsorption behaviour of the best-performing dispersant KV 5088, the slurry was titrated with 0.1 Polydadmac, a polyelectrolyte. At a given pH, the titration volume corresponds to the amount of ions present in the slurry due to the ionic dispersant. By centrifuging of the slurry the solvent (water) and the powder can be separated from each other. The back-titration of the centrifugate on the one hand and of the powder after redispersion in water on the other hand may reveal how much of the dispersant is attached to the powder surface. Figure 7 shows the polyelectrolyte titration curve of the slurry, of the redispersed powder and of the centrifuged solvent. It can be seen that the titration volumes of the slurry and of the redispersed powder are practically identical, whereas almost no dispersant was found in the centrifuged solvent. Moreover, in slurries the pH of which had been adjusted to 6 prior to centrifuging, the suspension of the redispersed powder showed a pH value shifted to about 8, which corresponds to the dissociation equilibrium of the dispersant. So it may be deduced that practically the whole amount of dispersant is adsorbed to the powder surface. Only at the more basic pH values does there seem to be a tendency of less adsorption, because some dispersant was found in the centrifuged solvent at pH 9-7.



(a)



(b)



(c)

Fig. 8. Scanning electron micrographs (SEM) of gelcast microstructures, with (a) dispersant KV 5088, (b) CE 64 and (c) PC 33.

### 3.4 Sintering and microstructures

Table 2 shows the resulting sintered densities according to the dispersant used for suspension in relation to the maximum solids loading. The aminoalcohol KV 5088 gave the best results and the

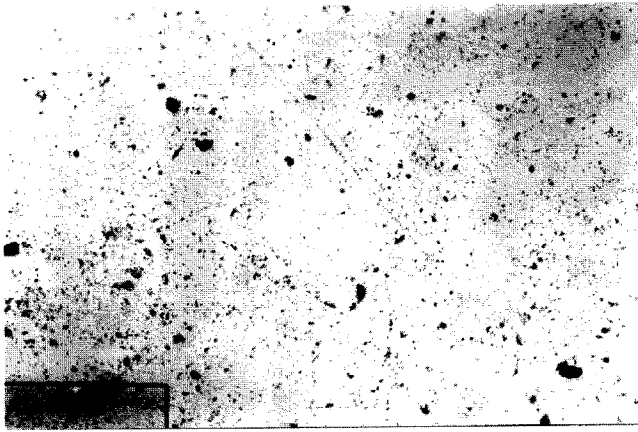


Fig. 9. Optical micrograph of the polished surface of gelcast TiN dispersed with KV 5088 — magnification 100  $\times$ .

sintered density reached 95.5% of the theoretical density, whereas the use of the two other dispersants led to strongly inhomogeneous microstructures and low sintering densities (Figs 8 a-c).

Figure 9 shows an optical micrograph of the polished microstructure of the TiN-sample dispersed with KV 5088 and a density of 95.5%. The dark spots within the microstructure are the residual porosity and the TiO<sub>2</sub> second phase. It can be seen that porosity and second phase are not homogeneously distributed and that areas within the microstructure are found, which contain less porosity than others and are obviously more dense. These microstructural inhomogeneities therefore reveal that the dispersion of the powder is still not ideal.

#### 4 Conclusions

Gelcasting of nanosized TiN was successfully carried out with a maximum solids loading of 22 vol% and a commercially available dispersant on the basis of an aminoalcohol. The limit of solids loading was found to be at 22 vol%. The rheological properties (structural viscosity) were positively influenced by both ball milling of the slurry prior to casting and the presence of the acrylamide monomers. The density of the sintered body was measured to be 95% of the theoretical.

#### Acknowledgements

The authors would like to express their gratitude to Dr Rabe for helpful discussions, Dr Mücke for preparation of the micrographs and Mrs Krull, Dipl.-Ings Nicolaidis and Kunzmann for carrying out the measurements. They would like to express special thanks for the translational help of Robert Germar and Cathy Pinguet from Saint Gobain Recherche, Paris.

#### References

1. Young, A. C., Omatete, O. O. & Janney, M. A., Gelcasting of alumina *J. Am. Ceram. Soc.*, **74** (1991) 612–618.
2. Omatete, O. O., Janney, M. A. & Strehlow, R. A., Gelcasting — a new ceramic forming process. *Ceram. Bull.*, **70** (1991) 1641–1649.
3. Omatete, O. O., Tieggs, T. N. & Young, A. C., Gelcast reaction bonded silicon nitride composites. *Ceram. Eng. Sci. Proc.*, **12** (1991) 1257–1264.
4. Omatete, O. O., Bleier, A., Westmoreland, C. G. & Young, A. C., Gelcast zirconia–alumina composites. *Ceram. Eng. Sci. Proc.*, **12** (1991) 2084–2094.
5. Wäsche, R., Steinborn, G. & Zingaro, A., Gelcasting of alumina and alumina–SiC composites. *Silicates Industriels*, 1995, in press.
6. Omatete, O. O. & Bleier, A., Tailoring suspension flow for the gelcasting of oxide and nonoxide ceramics. *Mat. Res. Soc. Symp. Proc.*, **346** (1994) 357–363.
7. Blackburn, S. R., Egerton, T. A. & Jones, A. G., Vapour phase synthesis of nitride ceramic powders using a DC plasma. *Brit. Ceram. Proc.*, **91** (1991) 87–94.
8. Rabe, T. & Wäsche, R., Sintering behaviour of nanocrystalline titanium nitride powders. *Nanostructured Mater.*, **6** (1991) 357–360.
9. Wäsche, R., Steinborn, G. & Baader, F., Elektrokinetische Messungen zur Charakterisierung wäBriger nanodisperser TiN-Suspension. *Fortschrittsberichte der DKG*, **9**(5) (1995) 151–158.
10. Lin, W. & Yang, J.-M., Thermal stability of electroconductive TiN-reinforced silicon oxynitride composites. *J. Eur. Cer. Soc.*, **13** (1994) 53–60.
11. Gogotsy, Y. G. & Yoshimura, M., Oxidation of powdered and sintered TiN. *Proceedings of IUMRS-ICAM-93*, Tokyo 31 August–4 September 1995. (*Transactions of the Materials Research Soc. of Japan*, 1995).
12. Omatete, O. O., Tieggs, T. N. & Young, A. C., Gelcast reaction bonded silicon nitride composites. *Ceram. Eng. Sci. Proc.*, **12** (1991) 1257–1264.
13. Dransfield, G. P. & Jones, A. G., The pressureless sintering of an ultra-fine plasma synthesized titanium nitride powder. *Euro-Ceramics II*, **1** (1991) 529–533.
14. Rabe, T. & Wäsche R., Development of dense nanocrystalline titanium nitride. *Ceram. Trans.*, **51** (1995), 531–535.